ACS OMEGA

http://pubs.acs.org/journal/acsodf

Article

Effects of Coal-Fired Flue Gas Components on Mercury Removal by the Mechanochemical S-Modified Petroleum Coke

Anjun Ma, Shilin Zhao,* Hui Luo, Kang Sun, Hesong Li, Yanqun Zhu, and Zhiqiang Sun*

Cite This: *ACS Omega* 2022, 7, 31205−31217

Read Online

ACCESS | Metrics & More | Article Recommendations

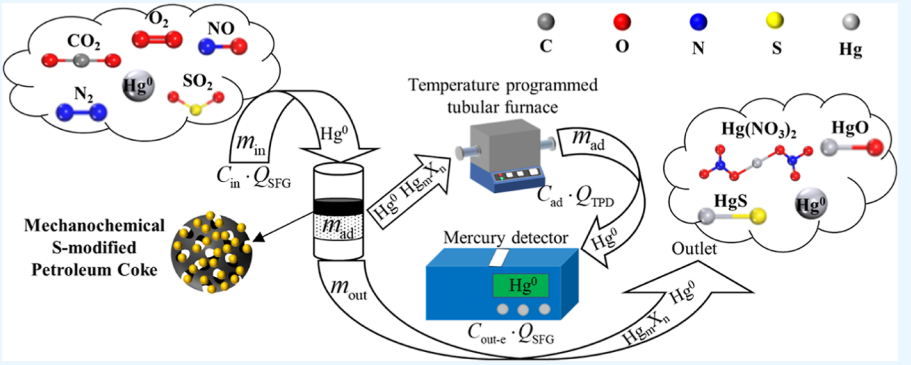

ABSTRACT: In this work, the effects of coal-fired flue gas components (O_2, CO_2, SO_2, and NO) on the Hg^0 removal by the promising mercury removal adsorbent mechanochemical S-modified petroleum coke were characterized and analyzed in terms of the Hg^0 removal efficiency, mercury adsorption capacity, and mercury mass balance. The results show that the mechanochemical S-modified petroleum coke with a theoretical sulfur content of 21% (named TSC-21) is the best candidate for mercury removal based on the Hg^0 removal efficiency, Hg^0 removal capacity, and difference ratio of Hg^0 removal capacity (anti-interference ability) in the basic and full-component simulated flue gas atmosphere ($N_2 + O_2 + CO_2$, $N_2 + O_2 + CO_2 + SO_2 + NO$). The maximum value (MV) and stable value (SV) of the Hg^0 removal efficiency of TSC-21 in the basic simulated flue gas atmosphere are 99.25% (MV) and 91.17% (SV), respectively. O_2, CO_2, and NO all promote the Hg^0 removal by the adsorbent, but they benefit the Hg^0 oxidation while inhibiting the Hg^0 adsorption. The promoting effect of O_2 on the Hg^0 removal by TSC-21 is affected by the reaction time, which is especially obvious after 1 min. The presence of SO_2 inhibits the oxidation and adsorption of Hg^0, which in turn reduces the Hg^0 removal performance of the adsorbent. The improving effects on the oxidative escape of Hg^0 by CO_2 is higher than that by NO and O_2. TSC-21 acts more as an oxidant than an adsorbent for Hg^0 removal.

1. INTRODUCTION

Mercury emitted from coal combustion has attracted worldwide attention due to its high toxicity, volatility, environmental persistence, and biomass accumulation. Coal-fired power plants are considered one of the major anthropogenic emission sources of atmospheric mercury.[1−3] Mercury in coal-fired flue gas exists in three forms, including elemental mercury (Hg^0), oxidized mercury (Hg^{2+},) and particle mercury (Hg^P).[4,5] Hg^P and Hg^{2+} can be captured using the dust removal unit (an electrostatic precipitator or a bag filter) and wet flue gas desulfurization system, respectively.[6,7] However, Hg^0 is difficult to be removed and easily escapes into the atmosphere because of its volatility and insolubility.[8,9] The activated carbon injection (ACI) technology is considered to be a mature technology for mercury removal from coal-fired flue gas, while the high operation cost limits its wide application.[10−13]

Replacing activated carbon with inexpensive, high-performance adsorbents is a relatively common approach to reducing the cost of ACI technology. As a byproduct of the delayed coking process, the petroleum coke is usually considered as an economical and promising precursor of carbon-based adsorbents.[14] Xiao et al.[15,16] brominated petroleum coke using mechanochemical methods and found that the mercury removal efficiency of raw petroleum coke (RPC) was greatly improved with the highest value of above 99%. Chen et al.[17] used the density functional theory to analyze the mercury removal mechanism by brominated petroleum coke. It found that bromine on the petroleum coke surface enabled HgO and

Received: June 2, 2022
Accepted: August 10, 2022
Published: August 25, 2022

https://doi.org/10.1021/acsomega.2c03449
ACS Omega 2022, 7, 31205−31217

Table 1. Proximate and Elemental Analysis of the High-Sulfur Petroleum Coke[a]

proximate analysis (wt %)				elemental analysis (wt %)					
M_{ad}	A_{ad}	V_{ad}	FC_{ad}	C_d	H_d	O_d	N_d	S_d	Cl_d
0.52	0.19	9.83	89.46	87.30	3.49	1.90	1.23	5.89	0.01

[a]Note: ad, air-dried basis; d, dried basis.

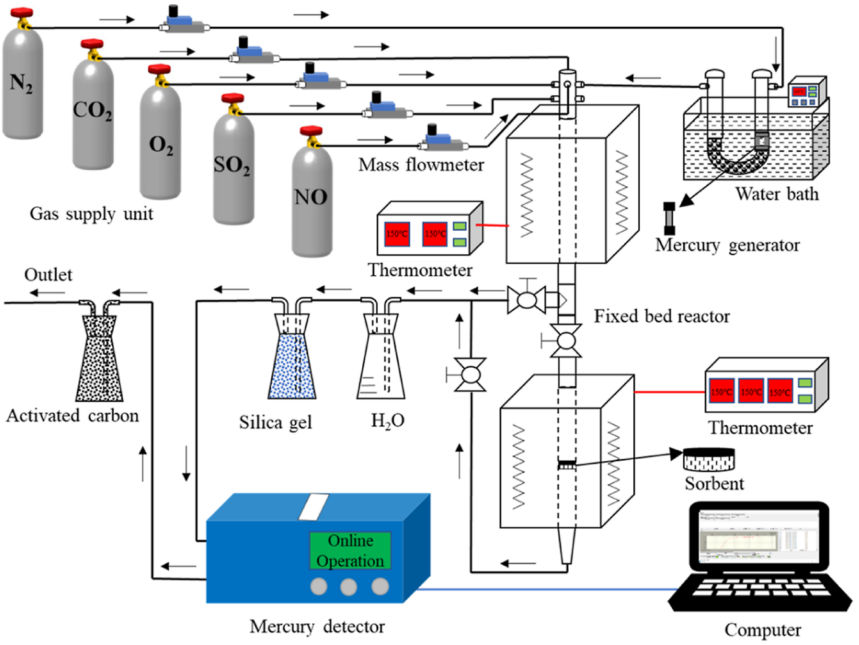

Figure 1. Schematic diagram of the SFG fixed bed mercury removal experimental device.

HgBr to be generated easily due to the increase of their adsorption energy and the decrease of their activation energy. She et al.[18] used the SO_2 high-temperature impregnation method to modify petroleum coke, due to which the mercury adsorption capacity of the adsorbent increased from 3.41 to 29.54−58.08 μg/g. Zhu et al.[19] prepared the columnar elemental sulfur-impregnated activated petroleum coke. It was found that the elemental sulfur impregnation was dominant for Hg^0 adsorption. Therefore, it can be seen that either bromine or sulfur modification can improve the mercury removal performance of RPC. For the bromine modification, the relatively higher cost and easy production of secondary pollution are the drawbacks of this method.[20,21] Mechanochemistry is a relatively novel and ideal modification method with the advantages of being a simple process, solvent-free, environmentally friendly, and highly efficient.[22,23] However, it is rarely used in the preparation of a petroleum coke-based mercury removal adsorbent combined with sulfur-containing modifiers. Based on our previous work,[24] the mechanochemical S-modified petroleum coke was a promising adsorbent for mercury removal from coal-fired flue gas. Zhang et al.[25] characterized the effects of the flue gas component on mercury removal by a sulfur-containing sorbent (used-Fe/SC120) at 90 °C, which indicated that O_2 and SO_2 inhibited the Hg^0 removal due to the lost active sulfur sites and competitive adsorption, which was beneficial for NO in improving the Hg^0 oxidation. Ma et al.[26] investigated the mercury removal performance of acid-treated activated coke at 160 °C in different flue gas atmospheres, which showed that NO could promote the mercury removal, while SO_2 had varied influences. Huang et al.[11] carried out the mercury removal with bromide (NH_4Br)-modified rice husk-activated carbon on a pilot-scale 0.3 MW circulating fluidized bed system. It found that increasing SO_2 concentration inhibited the mercury removal efficiency, whereas higher NO concentration promoted that. Xu et al.[27] used the pyrolysis method to prepare the biomass adsorbent modified by the brominated flame retarded, which found that SO_2, NO, O_2, and HCl were favorable for the mercury removal. Li et al.[28] synthesized sulfur-abundant S/FeS_2 by the hydrothermal method to remove the Hg^0 from coal-fired flue gas at low temperature. This indicated that the presence of 50−150 ppm SO_2 or 75 ppm NO had negligible effects on mercury removal by the adsorbent. Li et al.[29] studied the influence of acidic gases (CO_2, SO_2, NO, and HCl) on mercury removal by a raw activated carbon, which showed that NO and HCl could improve the mercury removal, while SO_2 was the negative factor. It can be seen that there have been some studies on the influence of flue gas components on the mercury removal performance by the adsorbents. NO, O_2, and HCl have a certain promoting effect on the mercury removal, while the influence of SO_2 on that is doubtful. In fact, the effects of flue gas components on the mercury removal performance of adsorbents are related to the adsorption temperature, the concentration of flue gas components, and so on. Therefore, it is necessary to investigate the influence of flue gas components on the mechanochemical S-modified petroleum coke adsorbent developed in our previous work.[24]

In this work, the effects of coal-fired flue gas components on mercury removal by the mechanochemical S-modified petroleum coke were characterized on a simulated flue gas (SFG) fixed bed mercury removal test bench, which were

https://doi.org/10.1021/acsomega.2c03449
ACS Omega 2022, 7, 31205−31217

analyzed in terms of Hg^0 removal efficiency, mercury adsorption capacity, and the mercury mass balance. The mercury temperature-programed desorption (Hg-TPD) analysis was used to obtain the mercury speciation and mercury adsorption on adsorbents after use.[30] The main contents include (1) screening of optimal mechanochemical S-modified petroleum coke; (2) effect of each flue gas component on mercury removal performance; and (3) comparative analysis based on the mercury mass balance. The main purpose is to comprehensively evaluate the mercury removal performance of mechanochemical S-modified petroleum coke and provide technical support and theoretical guidance for its industrial application.

2. EXPERIMENTAL SECTION

2.1. Sample Preparation. A kind of high-sulfur petroleum coke was selected to be the precursor of the mercury removal adsorbent, the proximate and elemental analyses of which are shown in Table 1. It is shown that carbon is the main content, and the sulfur content (5.89 wt %) is high. This facilitates the preparation of high-performance mercury removal adsorbents.[31] The high-sulfur petroleum coke was modified with the elemental sulfur (S) having a purity greater than 99.9% using the mechanochemical preparation method. The omni-directional planetary ball mill was the main equipment in the sample preparation process. The rotation speed of 600 rpm, the revolution speed of 300 rpm, and the milling time of 60 min were selected for the adsorbent preparation. The material of the grinding ball was zirconia, and the mass ratio of balls to the mixture of high-sulfur petroleum coke and S was 15:1. The theoretical sulfur content (TSC) was used as the basis for the quantification of high-sulfur petroleum coke and S in the mechanochemical S-modified petroleum coke adsorbent. It was defined as the ratio of the sum mass of sulfur in the petroleum coke and the modifier to the sum mass of the petroleum coke and the modifier, given in percentage. In this work, the mechanochemical S-modified petroleum coke adsorbents with different TSCs were prepared, which were named as TSC-9, TSC-13, TSC-17, TSC-21, and TSC-25, respectively. For example, TSC-9 represented the mechanochemical S-modified petroleum coke adsorbent for which the TSC was 9%.

2.2. Mercury Removal Test. The schematic diagram of the SFG fixed bed mercury removal experimental device is shown in Figure 1. It consisted of a gas supply unit, a mercury generator, a flue gas preheater, a fixed bed reactor, a system for online monitoring of Hg^0, and an exhaust gas treatment unit. Several mass flow meters (Beijing Sevenstar D07-19B, China) were used to control the flow rate of the SFG. The Hg^0 concentration was measured and recorded using the online mercury concentration analyzer (Lumex RA-915M, Canada). The flow rate of the SFG was set as 1 L/min, and the initial Hg^0 concentration was 51.5 ± 1.5 $\mu g/m^3$. The air velocity was about 0.15 m/s in the fixed bed. The amount of the adsorbent used for each set of mercury removal experiment was 100 mg, the particle size of which was about 200−400 μm. In the experimental process, N_2 was used to carry Hg^0 and balance the total flow. The temperatures of the preheated SFG and Hg^0 adsorption were all kept at 150 °C.

The experimental conditions designed in this work are shown in Table 2. The component of SFG-1 was a basic SFG under the ideal combustion condition of carbon and air, which included only N_2, O_2, and CO_2. The component of SFG-2 was the full-component SFG, in which the concentrations of O_2, CO_2, SO_2, and NO are all typical values for the coal combustion.[1,32,33] SFG-1 and SFG-2 were selected for the screening of the optimal mechanochemical S-modified petroleum coke. The operating conditions of SFG-3 to SFG-7 were used to study the effect of each flue gas composition on the mercury removal performance of the optimal mechanochemical S-modified petroleum coke.

Table 2. Experimental Conditions Designed in This Work

no.	simulated flue gas components
SFG-1	N_2 + 6% O_2 + 12% CO_2
SFG-2	N_2 + 6% O_2 + 12% CO_2 + 800 ppm SO_2 + 250 ppm NO
SFG-3	N_2
SFG-4	N_2 + 6% O_2
SFG-5	N_2 + 12% CO_2
SFG-6	N_2 + 800 ppm SO_2
SFG-7	N_2 + 250 ppm NO

2.3. Evaluation Index and Relevant Characterizations. Hg^0 removal efficiency and Hg^0 removal capacity were adopted to evaluate the mercury removal performance of the adsorbent, which are defined in Formulas 1 and 2 shown as follows.

$$\eta_t = \frac{C_{in} - C_{out-e}}{C_{in}} \times 100\% \quad (1)$$

$$q_t = \frac{Q_{SFG}}{m_{coke}} \int_0^{t_1} (C_{in} - C_{out-e}) dt \quad (2)$$

where η_t represents the Hg^0 removal efficiency, given in percentage; q_t represents the Hg^0 removal capacity, given in micrograms per gram; C_{in} and C_{out-e} represent the Hg^0 concentrations at the inlet and outlet of the fixed bed, respectively, given in micrograms per cubic meter; Q_{SFG} represents the total flow of the SFG, given in cubic meters per minute; m_{coke} represents the mass of the adsorbent, given in grams; and t_1 represents the time for the mercury removal, given in minutes.

For the screening of the optimal mechanochemical S-modified petroleum coke in the atmosphere of SFG-1 and SFG-2, the difference ratio of Hg^0 removal capacity was introduced, as shown in Formula 3.

$$r = \frac{q_{SFG-1} - q_{SFG-2}}{q_{SFG-1}} \times 100\% \quad (3)$$

where r represents the difference ratio of Hg^0 removal capacity, given in percentage and q_{SFG-1} and q_{SFG-2} represent the Hg^0 removal capacities in the atmospheres of SFG-1 and SFG-2, respectively, given in micrograms per gram.

For the influence of O_2, CO_2, SO_2, and NO on the mercury removal performance of the typical sample, the Hg-TPD test was carried out. The temperature-programed furnace (OTF-1200X, China) and the on-line mercury concentration analyzer (Lumex RA-915M, Canada) were used to analyze the mercury forms form the same adsorbent in different atmospheres. The samples were heated from room temperature to 700 °C with a heating rate of 5 °C/min in the temperature-programed furnace in N_2 with a flow rate of 100 mL/min. According to the Hg-TPD curve, the mercury adsorption capacity could be calculated based on Formula 4.

https://doi.org/10.1021/acsomega.2c03449
ACS Omega 2022, 7, 31205−31217

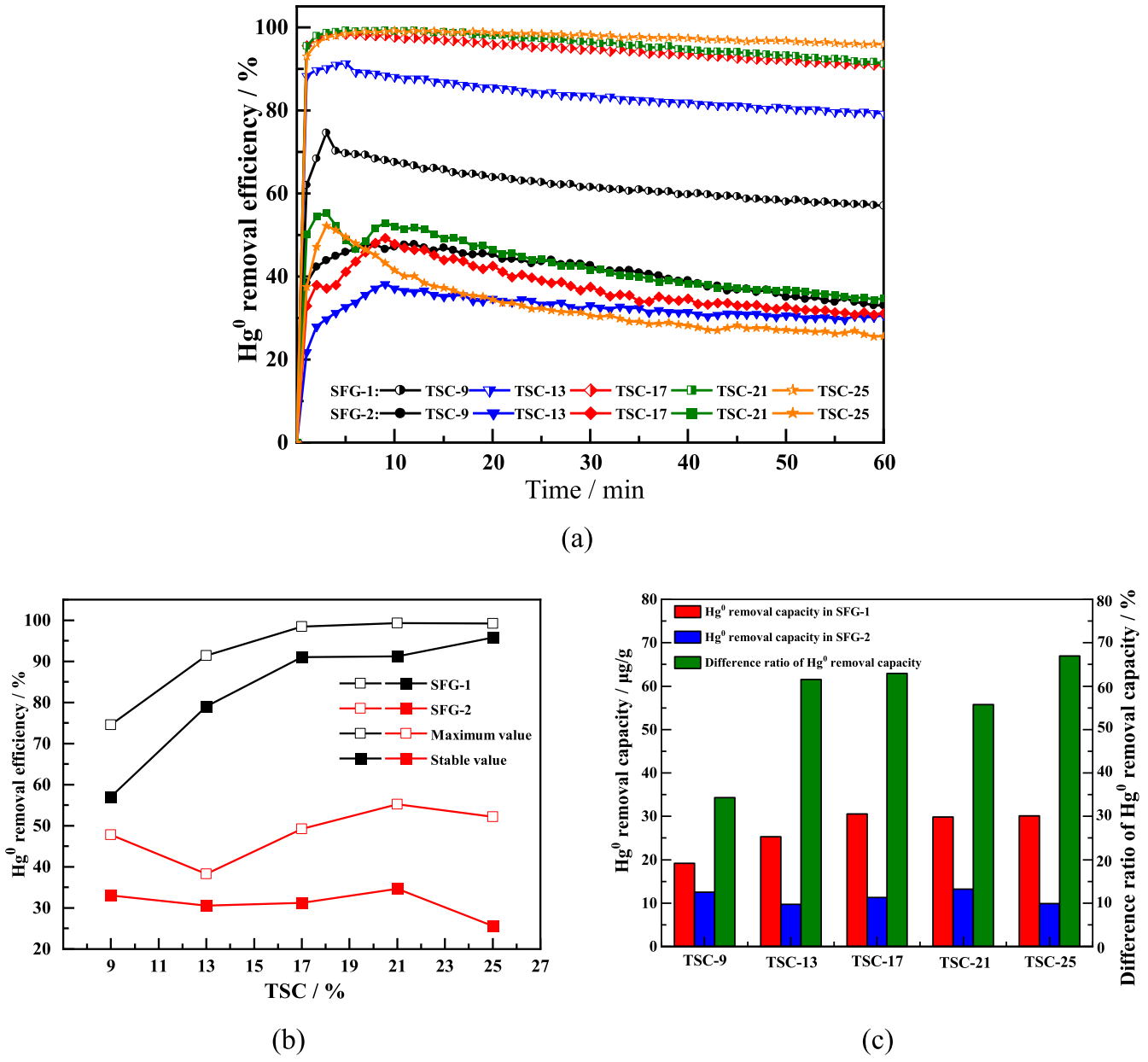

Figure 2. Mercury removal performance of mechanochemical S-modified petroleum coke with different TSCs in the atmospheres of SFG-1 and SFG-2. (a) Hg^0 removal efficiency vs time; (b) Maximum and stable values of Hg^0 removal efficiency vs TSC; and (c) Hg^0 mercury removal capacity and difference ratio vs TSC.

$$q_a = \frac{Q_{TPD}}{m_{coke}} \int_0^{t_2} C_{ad} dt \quad (4)$$

where q_a represents the amount of Hg^0 released during the Hg-TPD test, given in micrograms per gram; C_{ad} represents the Hg^0 concentration released from the adsorbent in the Hg-TPD process, given in micrograms per cubic meter; Q_{TPD} represents the flow of N_2, given in cubic meters per minute; m_{coke} represents the mass of the adsorbent, given in grams; and t_2 represents the time of the Hg-TPD test, given in minutes.

3. RESULTS AND DISCUSSION

3.1. Screening of the Optimal Mechanochemical S-Modified Petroleum Coke. The mercury removal performance of mechanochemical S-modified petroleum coke with different TSCs in the atmospheres of SFG-1 and SFG-2 is shown in Figure 2. From Figure 2a, Hg^0 removal efficiency of mechanochemical S modified petroleum coke with different TSCs achieves the maximum value (MV, 74.58−99.25%) quickly and decreases smoothly to their respective stable value (SV, about 57.00−96.80%) in the atmosphere of SFG-1. Both the MV and SV of Hg^0 removal efficiency of the adsorbent change regularly with the increase of TSC in the atmosphere of SFG-1. However, the MV and SV of the Hg^0 removal efficiency of the adsorbent do not have obvious regularity with the increase in the TSCs in the atmosphere of SFG-2. This indicates that the mercury removal performance of the adsorbent is affected by the full-component SFG. For the SFG-2 atmosphere, the Hg^0 removal efficiency of TSC-21 is slightly higher than that of TSC-9 in the initial reaction stage (within about 20 min) and then is almost the same with further increase in the reaction time. This shows that the excess

https://doi.org/10.1021/acsomega.2c03449
ACS Omega 2022, 7, 31205−31217

Table 3. Comparison of Mercury Removal Performance between Modified Carbon-Based Adsorbents and TSC-21

sample	precursor	modifier	preparation method	mercury removal conditions	η_t %	ref
40ZIS/CN	g-C_3N_4 nanosheet	$ZnIn_2S_4$	impregnation	~82.7 $\mu g/m^3$ Hg^0, N_2, 120 °C	~98.87%,	36
BC-8S_2Cl_2-IM	sawdust coke	S_2Cl_2	impregnation	50 $\mu g/m^3$ Hg^0, N_2 + 6% O_2 + 12% CO_2, 150 °C	91.94%	37
1M-500	sewage sludge	$ZnCl_2$	impregnation and pyrolysis	70 $\mu g/m^3$ Hg^0, N_2, 140 °C	~96.5%	38
FA-MC-Br	fly ash	NH_4Br	mechanochemistry	54 $\mu g/m^3$ Hg^0, N_2 + 4% O_2, 150 °C	~88%	39
TSC-21	petroleum coke	elemental sulfur	mechanochemistry	51.5 $\mu g/m^3$ Hg^0, N_2 + 6% O_2 + 12% CO_2, 150 °C	~99.25%	this work

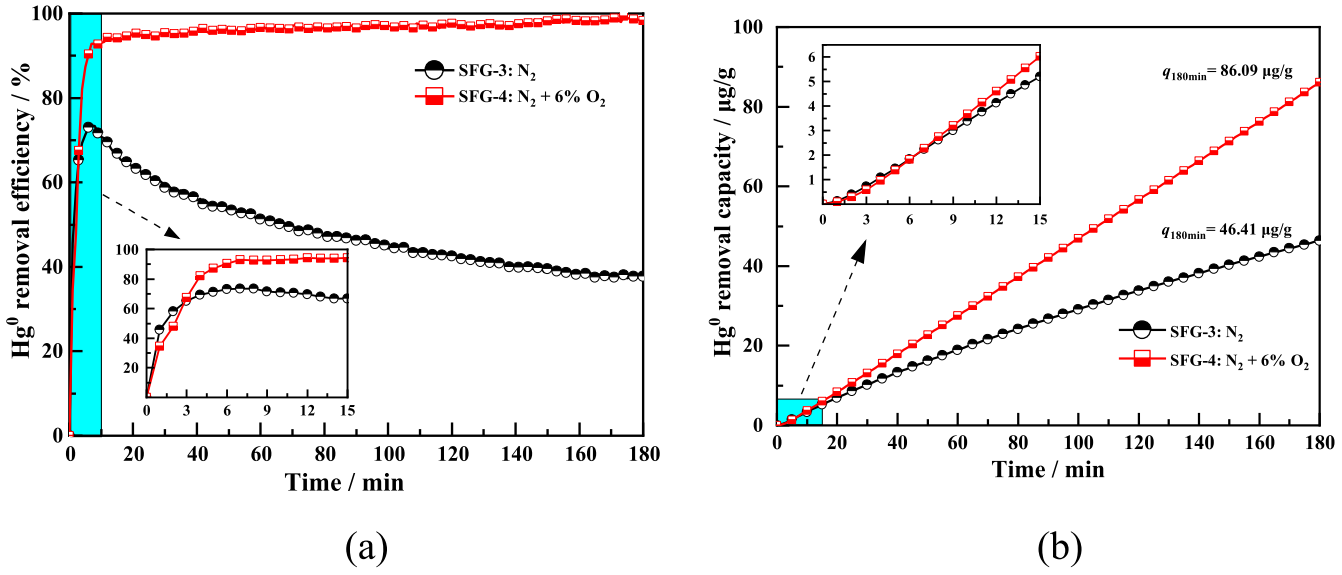

Figure 3. Effect of O_2 on the mercury removal performance of TSC-21. (a) Hg^0 removal efficiency vs time and (b) Hg^0 removal capacity vs time.

S addition does not significantly improve the mercury removal ability of the adsorbent, which is also reflected in the SFG-1 atmosphere. Comparing the Hg^0 removal efficiencies of TSC-9 and TSC-21 in the SFG-1 and SFG -2 atmospheres, it can be seen that 800 ppm SO_2 and 250 ppm NO have a more obvious inhibitory effect on the mercury removal ability of TSC-21, which may originate from the high SO_2 concentration in the SFG-2 atmosphere.[34,35] The excessive addition of the S modifier can increase the surface active sites of the adsorbent while also deteriorating the surface pore structure. The high concentration of SO_2 in the SFG-2 atmosphere may form SO_4^{2-} under the action of surface active sites (such as oxygen-containing functional groups) and O_2 in the flue gas, which hinders the Hg^0 removal by the active sites. These results in the lower SV of Hg^0 removal efficiency of TSC-25 in the SFG-2 atmosphere. From Figure 2b, the increase in the amplitude of the Hg^0 removal efficiency of the adsorbent with the TSC increasing from 9 to 17% changes obviously from 74.58% (MV) and 57.00% (SV) to 98.47% (MV) and 91.00% (SV), respectively, in the atmosphere of SFG-1, which will tend to be stable with a further increase in the TSC with the values of 98.47%−99.25% (MV) and 91.00%−95.80% (SV). For Hg^0 removal efficiency in the atmosphere of SFG-2, the changing ranges of the MV and SV are relatively smaller with the increase of TSC, which are 47.79−55.23% and 25.60−34.70%, respectively. It can be seen that the presence of NO and SO_2 in the SFG not only reduces the mercury removal efficiency of the adsorbent but also causes the mercury removal performance of the adsorbent to be irregular with the increase of TSC.

The Hg^0 mercury removal capacity and difference ratio of the adsorbent with different TSCs is summarized in Figure 2c, which shows that the difference ratio of Hg^0 removal capacity follows the order of TSC-9 (34.34%) < TSC-21 (55.74%) <TSC-13 (61.51%) <TSC-17 (62.92%) < TSC-25 (66.99%). The difference ratio of Hg^0 removal capacity of TSC-9 is the smallest one, while its mercury removal performance is much worse than that of the other samples. Considering the Hg^0 removal efficiency and removal capacity, TSC-21 is the relatively ideal adsorbent with a higher mercury removal performance [SFG-1: 99.25% (MV) and 91.17% (SV) and SFG-2: 55.23% (MV) and 34.69% (SV)] and a stronger anti-interference ability. Thus, TSC-21 is selected for the following study on the influence of flue gas components on the mercury removal performance.

In addition, the mercury removal work of some modified carbon-based adsorbents is listed in Table 3. It can be found that these modified carbon-based adsorbents can achieve the Hg^0 removal efficiency of about 90%, among which 40ZIS/CN, 1M-500, and TSC-21 all have the values of above 96%. In the case of similar mercury removal efficiency, mechanochemistry has a more convenient preparation method than impregnation or impregnation and pyrolysis, with a simple operation and a short preparation period. Comparing FA-MC-Br and TSC-21, it can be seen that the industrial byproduct petroleum coke has excellent potential as a support material for high-performance mercury removal adsorbents. Therefore, in view of the mercury removal ability, preparation method, and

https://doi.org/10.1021/acsomega.2c03449
ACS Omega 2022, 7, 31205−31217

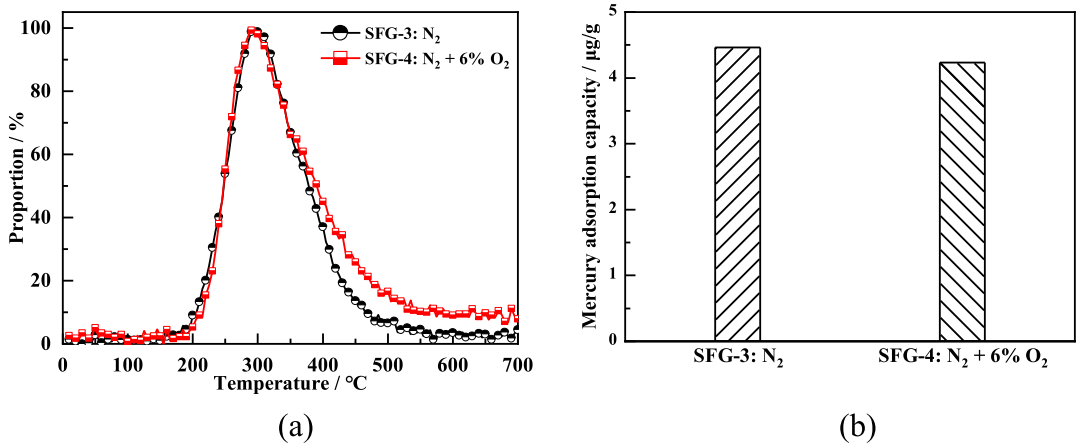

Figure 4. Hg-TPD results and mercury adsorption capacity of the used TSC-21 in SFG-3 and SFG-4. (a) Hg-TPD results and (b) mercury adsorption capacity.

support material, TSC-21 has a good application prospect for flue gas mercury removal.

3.2. Effect of Each Flue Gas Component on Mercury Removal Performance. *3.2.1. Effect of O_2.* The effect of O_2 on the mercury removal performance of TSC-21 is shown in Figure 3. In Figure 3a, it is shown that the presence of 6% O_2 improves the Hg^0 removal efficiency of TSC-21 in the N_2 atmosphere, which increases from 73.41% (MV) and 37.73% (SV) in SFG-3 to 99.37% (MV) and 98.32% (SV) in SFG-4. The Hg^0 removal efficiency in the atmosphere of SFG-3 is higher than that in SFG-4 within the first 3 min, which both reach a large value at around 7 min in the two atmospheres. After 7 min, the Hg^0 removal efficiency of TSC-21 in the atmosphere of SFG-4 increases smoothly from 92.84 to 98.32% (SV), while that in the atmosphere of SFG-3 decreases relatively quickly from 73.41% (MV) to 37.73% (SV). In Figure 3b, it is shown that the Hg^0 removal capacity (86.09 μg/g) of TSC-21 in the atmosphere of SFG-4 is nearly 2 times that (46.41 μg/g) in SFG-3 within the reaction time of 180 min. The reason of this promotion effect in the presence of O_2 is the heterogeneous reaction between Hg^0 and O_2 occurring on the adsorbent surface.[40] Moreover, the Hg^0 removal capacity of TSC-21 in the atmosphere of SFG-4 within the first 7 min is lower than that in the atmosphere of SFG-3. It can be found that the reaction time is an important factor affecting O_2 in promoting or inhibiting the Hg^0 removal performance of TSC-21. This may be due to the competitive adsorption of O_2 and Hg^0 on the adsorbent surface in the initial stage under the O_2 atmosphere, which inhibits the contact of Hg^0 with the adsorbent surface. After 3 min, the adsorbed O_2 has been transformed to active sites favorable for the Hg^0 oxidation on the adsorbent surface, which thereby enhances its mercury removal ability.

The Hg-TPD results and mercury adsorption capacity of the used TSC-21 in SFG-3 and SFG-4 are shown in Figure 4. From Figure 4a, the obvious peak of the Hg-TPD curve in the two atmospheres occurs near 300 °C. According to previous research studies,[41−43] the mercury compound corresponding to this decomposition peak may be HgS or HgO. Considering the TSC-21 adsorbent containing a certain amount of sulfur, HgS should be the dominated mercury form. From Figure 4b, it is shown that the mercury adsorption capacity of TSC-21 in the atmosphere of SFG-4 (4.23 μg/g) is lower than that in the atmosphere of SFG-3 (4.46 μg/g). For the SFG-3 atmosphere, the Hg^0 removal capacity of TSC-21 (46.41 μg/g) is much larger than its mercury adsorption capacity (4.46 μg/g), which indicates that a large amount of Hg^0 is oxidized in the mercury removal process in the N_2 atmosphere. This may be caused by the presence of oxygen-containing functional groups on the adsorbent surface [such as C−O and C−O−C (1250−1500 cm^{-1}) and C═O (1500−1750 cm^{-1}),[15] as shown in Figure 5.[44] Combining with Figures 3 and 4, it can be seen that the

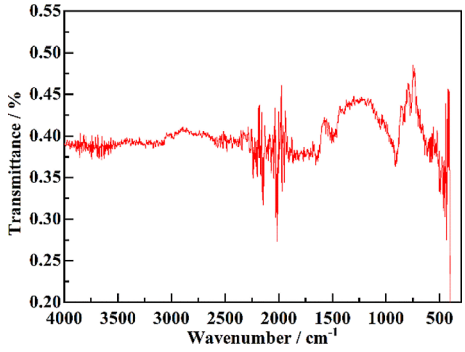

Figure 5. Fourier transform infrared spectra of TSC-21.

presence of O_2 is beneficial for the improvement of the mercury removal performance of TSC-21 (including Hg^0 removal efficiency and Hg^0 removal capacity), where the mercury adsorption capacity of TSC-21 in the SFG-3 atmosphere is higher than that in the SFG-4 atmosphere. This shows that the existence of O_2 mainly promotes the heterogeneous reaction of Hg^0 on the adsorbent surface, but the Hg^{2+} after the heterogeneous oxidation will leave the adsorbent and enter the flue gas leaving the fixed bed. Moreover, the presence of O_2 plays a dominate role in the Hg^0 oxidation process.

3.2.2. Effect of CO_2. The effect of CO_2 on the mercury removal performance of TSC-21 is shown in Figure 6. It can be seen that the presence of CO_2 is beneficial for the improvement of the mercury removal performance of TSC-21, where Hg^0 removal efficiency (MV, 96.72%) and Hg^0 removal capacity (80.71 μg/g) in SFG-5 is higher than that in SFG- 3. As shown in Figure 6a, the Hg^0 removal efficiency of TSC-21 in the atmosphere of SFG-5 quickly reaches 96.72% (MV) and then slowly decreases to 71.57% (SV). The Hg^0 removal efficiency of the two atmospheres is similar before 1

https://doi.org/10.1021/acsomega.2c03449
ACS Omega 2022, 7, 31205−31217

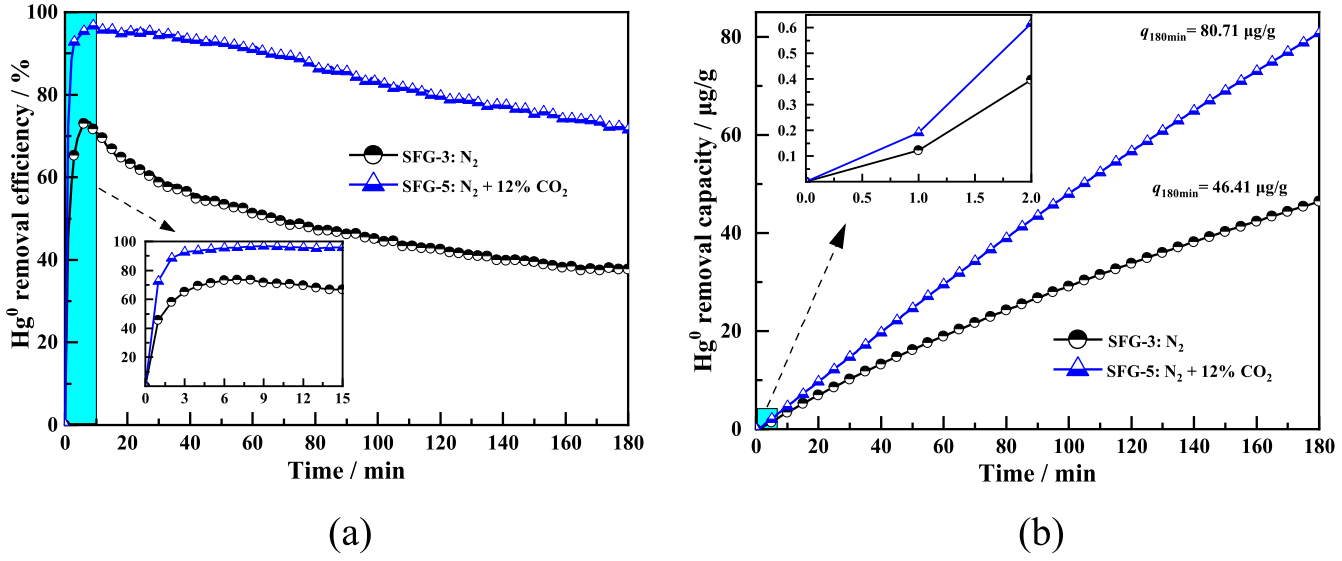

Figure 6. Effect of CO_2 on the mercury removal performance of TSC-21. (a) Hg^0 removal efficiency vs time and (b) Hg^0 removal capacity vs time.

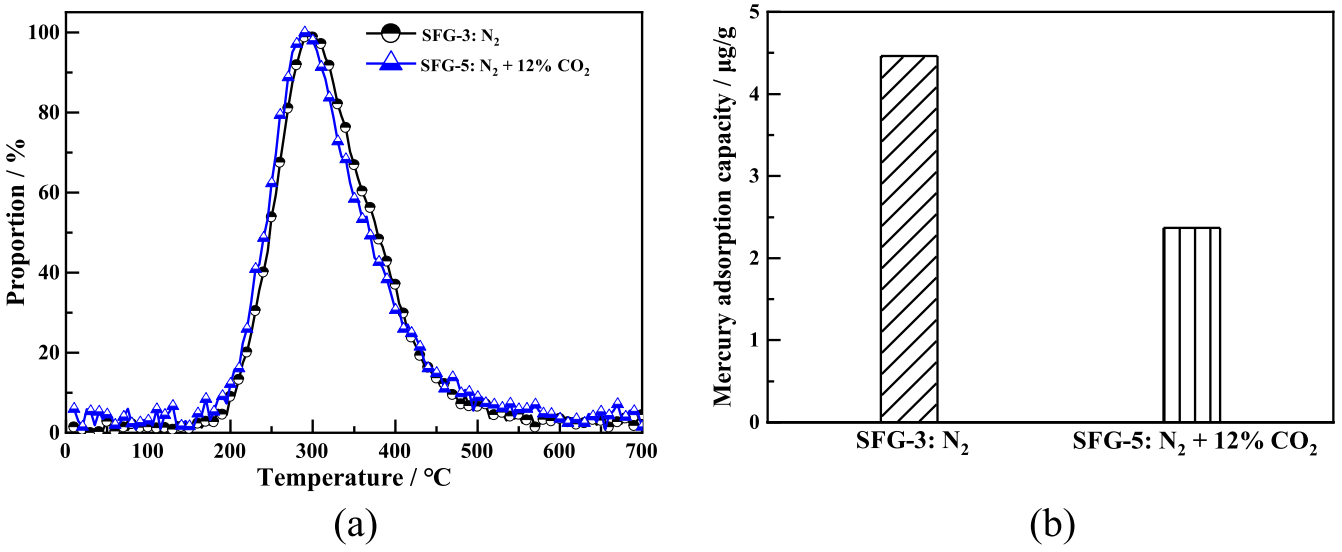

Figure 7. Hg-TPD results and mercury adsorption capacity of the used TSC-21 in SFG-3 and SFG-5. (a) Hg-TPD results and (b) mercury adsorption capacity.

min, but the promotion effect of CO_2 is obvious after 1 min. From Figure 6b, the Hg^0 removal capacity of TSC-21 in the SFG-3 and SFG-5 atmospheres has an inflection point at around 1 min, where the distance between them gradually widened with the increase in the reaction time after 1 min. Therefore, the promoting effect of CO_2 on the Hg^0 removal of TSC-21 is not affected by the reaction time.

The Hg-TPD results and mercury adsorption capacity of the used TSC-21 in SFG-3 and SFG-5 are shown in Figure 7. From Figure 7a, the Hg-TPD curve of the used TSC-21 in the atmosphere of SFG-5 agrees well with that in the atmosphere of SFG-3. The peak temperature of the Hg-TPD curve in the two atmospheres is around 300 °C, which corresponds to HgS combined with the reaction conditions. Thus, the presence of CO_2 does not promote the generation of new mercury compounds, where HgS is still the main mercury form on the used TSC-21 in the atmosphere of SFG-5. From Figure 7b, the mercury adsorption capacity (2.37 μg/g) of TSC-21 in the SFG-5 atmosphere decrease obviously compared to that (4.46 μg/g) in the SFG-3 atmosphere. In the SFG-5 atmosphere, CO_2 will partially fill the surface microporous structure of the mechanochemical S-modified petroleum coke adsorbent on one hand, which inhibits the adsorption of flue gas mercury.[40] On the other hand, CO_2 will react with the carbon on the adsorbent surface to form oxygen-containing functional groups, which is favorable for Hg^0 oxidation.[40,45−47] Therefore, for mechanochemical S-modified petroleum coke, the presence of CO_2 promotes the Hg^0 oxidation on the adsorbent surface but inhibits the adsorption of flue gas mercury on the adsorbent. It results in the improvement of mercury removal ability of TSC-21 but a decrease in the mercury adsorption capacity.

3.2.3. Effect of SO_2. The effect of SO_2 on the mercury removal performance of TSC-21 is shown in Figure 8. From Figure 8a, the Hg^0 removal efficiency of TSC-21 decreases from 73.41% (MV) and 37.73 (SV) in the SFG-3 atmosphere to 53.80% (MV) and 23.11% (SV) in the SFG-6 atmosphere. The curves of Hg^0 removal efficiency of TSC-21 in the two

https://doi.org/10.1021/acsomega.2c03449
ACS Omega 2022, 7, 31205−31217

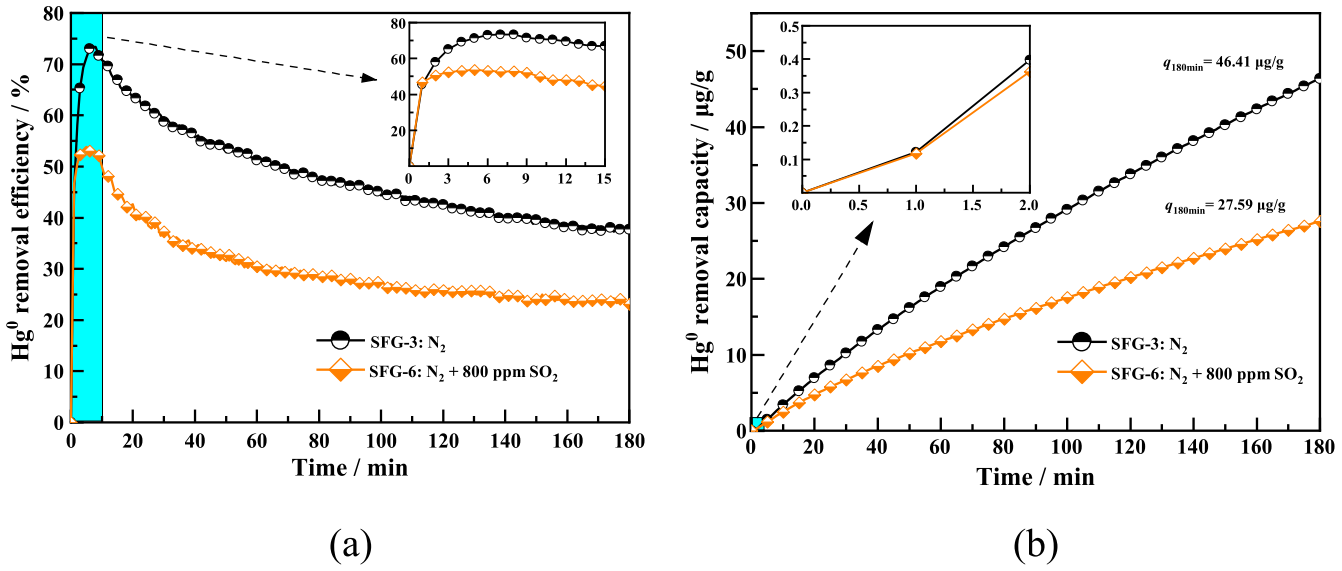

Figure 8. Effect of SO_2 on the mercury removal performance of TSC-21. (a) Hg^0 removal efficiency vs time and (b) Hg^0 removal capacity vs time.

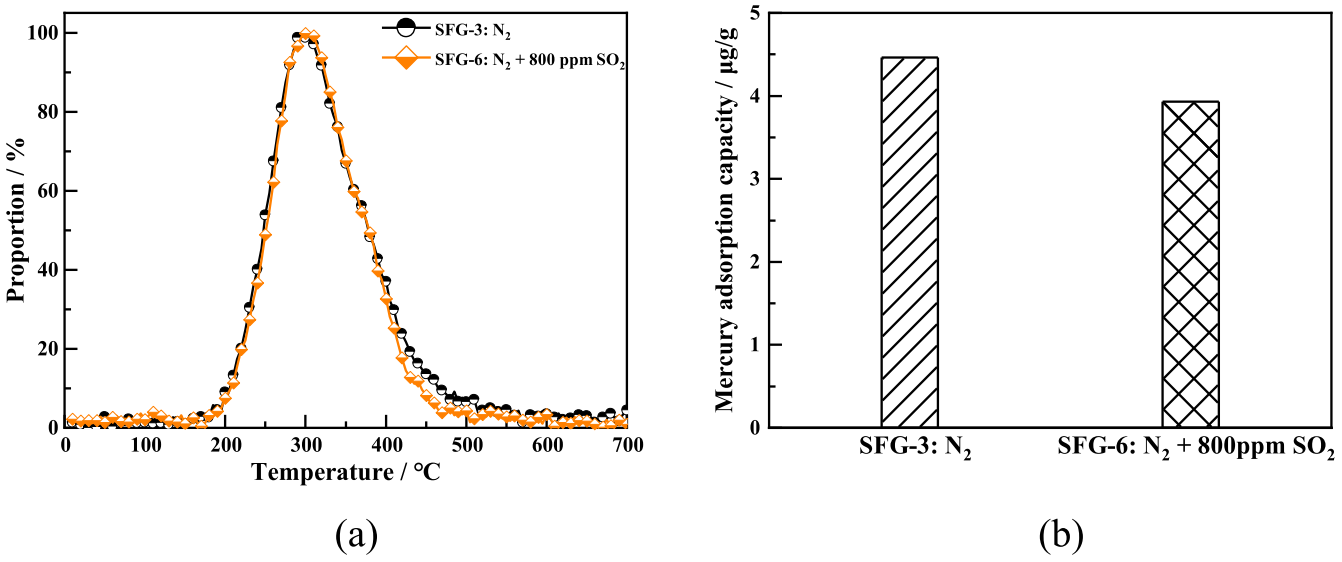

Figure 9. Hg-TPD results and mercury adsorption capacity of the used TSC-21 in SFG-3 and SFG-6. (a) Hg-TPD results and (b) mercury adsorption capacity.

atmospheres almost coincide within the first 1 min, which will reach the respective MV and SV at different changing rates after that. From Figure 8b, the Hg^0 removal capacity of TSC-21 decreases from 46.41 μg/g in the SFG-3 atmosphere to 27.59 μg/g in the SFG-6 atmosphere within the same reaction time of 180 min. There is the same inflection point at the reaction time of 1 min, which is also the demarcation point of Hg^0 removal capacity with different changing rates in the atmosphere of N_2 and N_2 + SO_2, respectively. Thus, the presence of SO_2 has a significant inhibitory effect on the mercury removal of mechanochemical S-modified petroleum coke, and the inhibitory effect is obvious after the reaction time of 1 min. This may be because there is a competitive adsorption between SO_2 and Hg^0 on the adsorbent surface in the initial stage, but the surface active sites still play a role in the mercury removal process. With the prolongation of the reaction time, the surface active sites are further covered. There also exists the reduction of oxidized mercury by SO_2, which leads to a significant decrease in the mercury removal ability.

The Hg-TPD results and mercury adsorption capacity of the used TSC-21 in SFG-3 and SFG-6 are shown in Figure 9. From Figure 9a, the Hg-TPD curves of the used TSC-21 in the two atmospheres of SFG-3 and SFG-6 have good similarities. The presence of SO_2 does not promote the generation of sulfur-containing mercury compounds, where HgS is still the main mercury compound on the used TSC-21 in the presence of SO_2. From Figure 9b, the mercury adsorption capacity (4.46 μg/g) of the adsorbent in the SFG-3 atmosphere is higher than that (3.93 μg/g) in the SFG-6 atmosphere. This shows that the presence of SO_2 can inhibit the flue gas mercury adsorption. The inhibitory effect of SO_2 on the mercury removal performance of mechanochemical S-modified petroleum coke may be due to the following reasons. (1) SO_2 competes with Hg^0 for adsorption on the adsorbent surface, which occupies part of the active sites for mercury removal.[25,48] (2) HgO

https://doi.org/10.1021/acsomega.2c03449
ACS Omega 2022, 7, 31205−31217

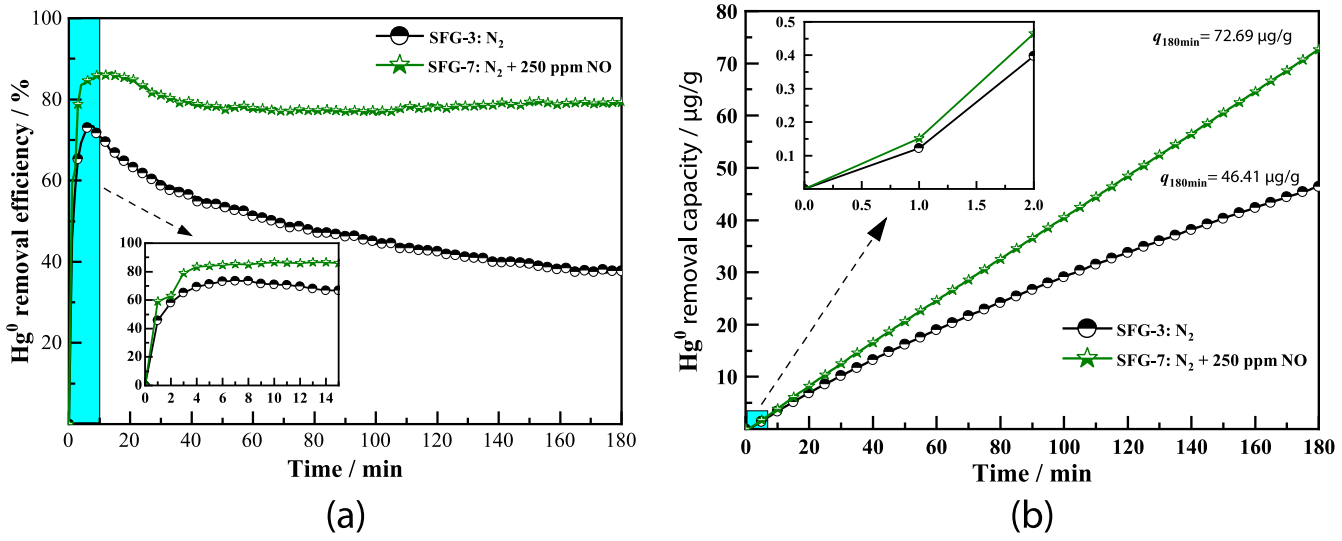

Figure 10. Effect of NO on the mercury removal performance of TSC-21. (a) Hg^0 removal efficiency vs time and (b) Hg^0 removal capacity vs time.

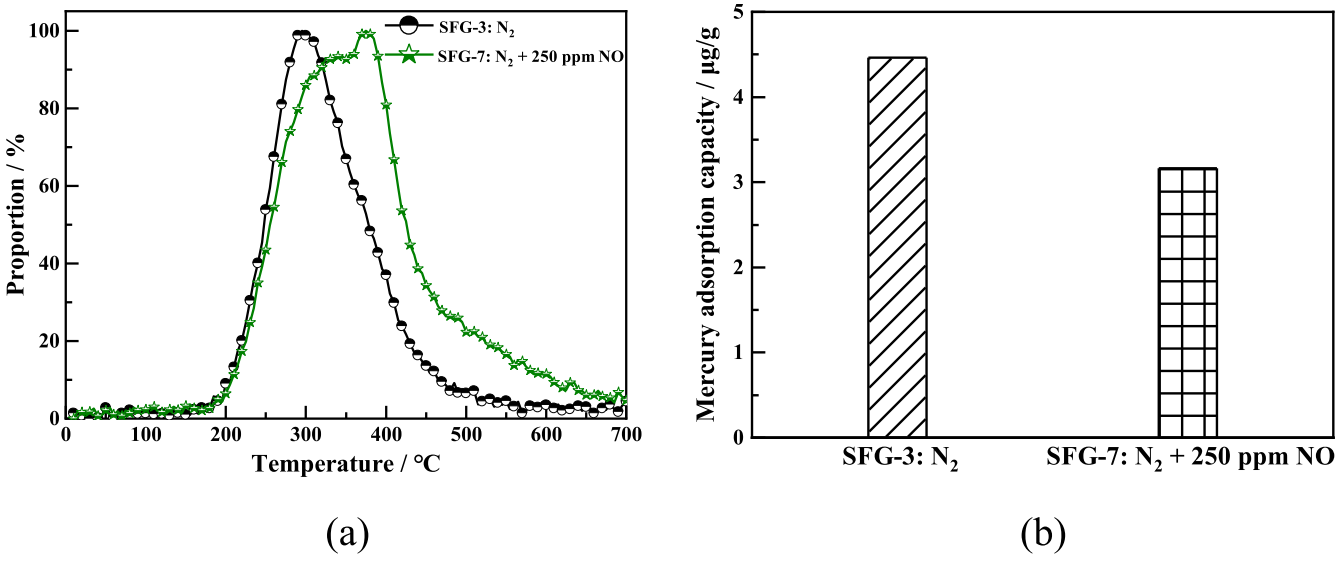

Figure 11. Hg-TPD results and mercury adsorption capacity of the used TSC-21 in SFG-3 and SFG-7. (a) Hg-TPD results and (b) mercury adsorption capacity.

generated by the reaction between Hg^0 and the oxygen functional group on the adsorbent surface can be reduced to Hg^0 by SO_2, as described in Formula 5.[29,49] The generated SO_3 will further inhibit the adsorption of Hg^0 on the adsorbent surface.[50] Compared to the Hg^0 removal capacity and mercury adsorption capacity of TSC-21 in the SFG-3 atmosphere, it can be found that the decrease (18.82 μg/g) in the Hg^0 removal capacity is higher than that (0.53 μg/g) in the mercury adsorption capacity in the SFG-6 atmosphere. This indicates that the presence of SO_2 reduces both the oxidation and adsorption of mercury, which leads to a decrease in the Hg^0 removal efficiency.

$$HgO(ad) + SO_2 \rightarrow Hg^0 + SO_3(ad) \quad (5)$$

3.2.4. Effect of NO. The effect of NO on the mercury removal performance of TSC-21 is shown in Figure 10. From Figure 10a, the presence of NO is beneficial for the improvement of the Hg^0 removal efficiency, which will increase from 73.41% (MV) and 37.73 (SV) in the SFG-3 atmosphere to 86.63% (MV) and 79.27% (SV) in the SFG-7 atmosphere. The main promoting effect on the increasing rate of Hg^0 removal efficiency occurs after the reaction time of 1 min. The Hg^0 removal efficiency of TSC-21 in the atmosphere of NO is stable in the range of 77%−80% after the reaction time of 30 min. From Figure 10b, the Hg^0 removal capacity (72.69 μg/g) in the atmosphere of SFG-7 is higher than that (46.41 μg/g) in the atmosphere of SFG-3 in the whole reaction process. There is also an inflection point in the Hg^0 removal capacity curve, which exists around the reaction time of 1 min. Similar to CO_2, the effect of NO on the mercury removal of TSC-21 is also not limited by the reaction time, which always has the positive factor for the mercury removal performance.

The Hg-TPD results and mercury adsorption capacity of the used TSC-21 in SFG-3 and SFG-7 are shown in Figure 11. From Figure 11a, it is shown that the Hg-TPD curve of the used TSC-21 in the SFG-7 atmosphere has two obvious peaks at around 312 °C and 375 °C, which usually correspond to HgO and/or HgS.[5,41,42] In addition, a small peak of the Hg-

https://doi.org/10.1021/acsomega.2c03449
ACS Omega 2022, 7, 31205−31217

TPD curve in the range of 445−500 °C in the SFG-7 atmosphere indicates that there is a relatively small proportion of $Hg(NO_3)_2$.[41,42] From Figure 11b, it can be found that the mercury adsorption capacity (3.16 μg/g) of TSC-21 in the SFG-7 atmosphere is still lower than that (4.46 μg/g) in the SFG-3 atmosphere. When NO exists in the SFG, NO will form NO_2 under the action of surface oxygen (O*) on the carbon-based adsorbent surface, and the NO_2 can promote the oxidation of mercury to form HgO and $Hg(NO_3)_2$, as shown in Formula 6 −8.[51] In addition, the generated mercury compound $Hg(NO_3)_2$ has a certain volatility.[52] Therefore, the addition of NO promotes the Hg^0 oxidation by the mechanochemical S-modified petroleum coke, while generating a more volatile mercury compound [$Hg(NO_3)_2$]. NO occupies the adsorption site of flue gas mercury on the adsorbent surface. This eventually led to an improvement in the mercury removal performance but a decrease in the mercury adsorption capacity.

$$2NO + O^* \rightarrow 2NO_2 \tag{6}$$

$$Hg^0 + NO_2 \rightarrow HgO + NO \tag{7}$$

$$2NO_2 + Hg^0 + O_2 \rightarrow Hg(NO_3)_2 \tag{8}$$

3.3. Comparative Analysis Based on the Mercury Mass Balance. The mercury mass balance for mercury removal by the adsorbent is established, which is shown in Figure 12. The mercury mass balance in the Hg^0 removal process can be described by Formulas 9 and 10.

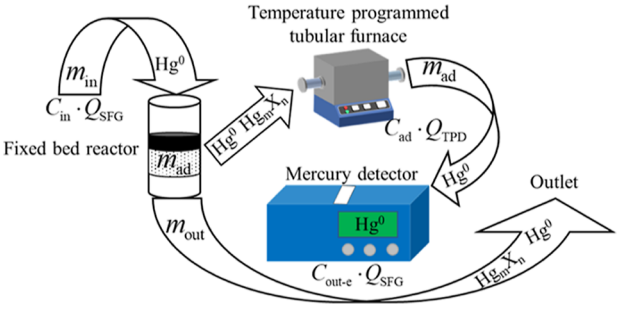

Figure 12. Schematic diagram of the mercury mass balance for mercury removal by the adsorbent.

$$m_{in} = m_{ad} + m_{out} \tag{9}$$

$$m_{out} = m_{out-e} + m_{out-ox} \tag{10}$$

where m_{in} represents the Hg^0 mass flow at the inlet of the fixed bed, given in micrograms per minute; m_{out} represents the mercury mass flow at the outlet of the fixed bed, given in micrograms per minute; m_{out-e} and m_{out-ox} represent the mass flow of Hg^0 and Hg^{2+} at the outlet of the fixed bed, respectively, given in micrograms per minute; and m_{ad} represents the mass of mercury adsorbed on the adsorbent per unit time, given in micrograms per minute.

Then, the amount of Hg^{2+} escaped is introduced and described by Formula 11.

$$q_o = \frac{m_{in} - m_{out-e} - m_{ad}}{m_{coke}} = \frac{Q_{SFG}}{m_{coke}} \int_0^{t_1} (C_{in} - C_{out-e})dt - \frac{Q_{TPD}}{m_{coke}} \int_0^{t_2} C_{ad}dt \tag{11}$$

The escaping rate of Hg^{2+} is introduced and described by Formula 12.

$$r_o = \frac{q_o}{q_t} \tag{12}$$

where q_o represents the escaping amount of Hg^{2+}, given in micrograms per gram and r_o represents the escaping rate of Hg^{2+}, given in percentage.

The mercury removal performances of TSC-21 in the atmospheres of SFG-3 to SFG-7 are summarized in Table 4. It shows that the escaping rates of Hg^{2+} in the five different atmospheres are 85.76−97.06%, where the rate in the N_2 + 12% CO_2 atmosphere has the highest value, while that in the N_2+ 800 ppm SO_2 atmosphere has the lowest value. Zhou et al.[30] conducted an experimental study on the effects of flue gas components on the oxidation and adsorption of Hg^0 by the NH_4Br-modified fly ash, which used 10% $SnCl_2$ to reduce the Hg^{2+} in the exhaust gas to Hg^0 and measured the Hg^{2+} concentration in the exhaust gas combined with the subtraction method. It also found a certain percentage of oxidative escaping mercury. The mercury adsorption capacities of TSC-21 in the five different atmospheres are 2.37−4.46 μg/g, which are all smaller than that in the pure N_2 atmosphere (4.46 μg/g). However, the Hg^{2+} escaping amounts in the five different atmospheres are in the range 23.66−81.86 μg/g, which is higher than the mercury adsorption capacity. For the mechanochemical S-modified petroleum coke, the poor surface structure is the main reason for its lower mercury adsorption capacity. The oxygen-containing functional groups and active sulfur on the adsorbent surface are the main internal reasons for its high Hg^0 oxidation ability. Overall, TSC-21 acts more as an oxidant than an adsorbent for Hg^0 removal. From the Hg^0 removal capacity (q_t), it can be seen that O_2, CO_2, and NO all promote Hg^0 removal by the mechanochemical S-modified petroleum coke, while SO_2 plays an inhibitory role. The escaping rate of Hg^{2+} (97.06%) in the N_2 + 12% CO_2 atmosphere is greater than that in the atmosphere of N_2 + 250 ppm NO (95.65%) ≈ N_2 + 6% O_2 (95.09%), which indicates that the improving effects on the oxidative escaping of Hg^0 by CO_2 is higher than that by NO and O_2. The Hg^0 removal capacity (80.71 μg/g) in the N_2 + 12% CO_2 atmosphere is larger than that (72.69 μg/g) in the atmosphere of N_2 + 250 ppm NO, while the mercury adsorption capacity on the adsorbent in the two atmospheres has the opposite trend. This further illustrates that CO_2 promotes the oxidation

Table 4. Mercury Removal Performance of TSC-21 in the Atmospheres of SFG-3 to SFG-7

no.	SFG components	q_t μg/g	q_a μg/g	q_o μg/g	r_o %
SFG-3	N_2	46.41	4.46	41.95	90.39
SFG-4	N_2 + 6% O_2	86.09	4.23	81.86	95.09
SFG-5	N_2 + 12% CO_2	80.71	2.37	78.34	97.06
SFG-6	N_2 + 800 ppm SO_2	27.59	3.93	23.66	85.76
SFG-7	N_2 + 250 ppm NO	72.69	3.16	69.53	95.65

https://doi.org/10.1021/acsomega.2c03449
ACS Omega 2022, 7, 31205−31217

of mercury but inhibits the adsorption of flue gas mercury on the adsorbent.

4. CONCLUSIONS

(1) Considering the Hg^0 removal efficiency, Hg^0 removal capacity, and difference ratio of Hg^0 removal capacity (anti-interference ability) in the SFG-1 and SFG-2 atmospheres, the mechanochemical S-modified petroleum coke adsorbent with the TSC of 21% is the best candidate for mercury removal. The MV and SV of Hg^0 removal efficiency of TSC-21 in the atmospheres of SFG-1 and SFG-2 are 99.25% (MV) and 91.17% (SV) and 55.23% (MV) and 34.69% (SV), respectively. O_2, CO_2, and NO all promote the Hg^0 removal by TSC-21, and the promotion effect of O_2 on Hg^0 removal is limited by the reaction time (there is an obvious promotion effect after the reaction time of 1 min). All these three components promote the Hg^0 oxidation on the TSC-21 surface but inhibit the adsorption of flue gas mercury on the adsorbent. SO_2 has an obvious inhibitory effect on the mercury removal from TSC-21 especially after 1 min of reaction time, which results from the decrease in both the oxidation and adsorption of Hg^0. The escaping rates of Hg^{2+} in the five different atmospheres (SFG-3 to SFG-7) are 85.76%−97.06%, and TSC-21 acts more as an oxidant than an adsorbent for Hg^0 removal. The improving effects on the oxidative escape of Hg^0 by CO_2 is higher than that by NO and O_2.

(2) In the follow-up research, the pore structure of the adsorbent should be improved as much as possible to provide more physical adsorption or chemical active sites to further improve the Hg^0 removal ability. Based on the position where the traditional ACI technology is used in the coal-fired power plant, the escaping of oxidized mercury will be captured by the subsequent dust collectors or wet desulfurization units. Therefore, it is necessary to comprehensively analyze the environmental stability, emission requirement, and reusability of fly ash and the used adsorbent, desulfurization wastewater, and desulfurization gypsum after mercury removal by the adsorbent injection, in addition to paying attention to the mercury concentration in the flue gas emitted to the atmosphere.

AUTHOR INFORMATION

Corresponding Authors

Shilin Zhao − *School of Energy Science and Engineering, Central South University, Changsha 410083, China; State Key Laboratory of Clean Energy Utilization, Zhejiang University, Hangzhou 310027, China;* orcid.org/0000-0002-5318-2042; Email: slzhao@csu.edu.cn

Zhiqiang Sun − *School of Energy Science and Engineering, Central South University, Changsha 410083, China;* Email: zqsun@csu.edu.cn

Authors

Anjun Ma − *School of Energy Science and Engineering, Central South University, Changsha 410083, China*

Hui Luo − *School of Energy Science and Engineering, Central South University, Changsha 410083, China*

Kang Sun − *School of Energy Science and Engineering, Central South University, Changsha 410083, China*

Hesong Li − *School of Energy Science and Engineering, Central South University, Changsha 410083, China*

Yanqun Zhu − *State Key Laboratory of Clean Energy Utilization, Zhejiang University, Hangzhou 310027, China;* orcid.org/0000-0002-0981-2078

Complete contact information is available at: https://pubs.acs.org/10.1021/acsomega.2c03449

Notes

The authors declare no competing financial interest.

ACKNOWLEDGMENTS

This work was financially supported by the National Natural Science Foundation of China [grant no. 52006245], the Science and Technology Innovation Program of Hunan Province [no. 2021RC4006], the Environmental Protection Research Project of Hunan Provincial Department of Ecology and Environment, the Natural Science Foundation of Hunan Province [grant no. 2021JJ40775], the Postgraduate Research and Innovation Project of Central South University [grant no. 2021zzts0154], the Innovation-Driven Project of Central South University [grant no. 2020CX008], and the State Key Laboratory of Clean Energy Utilization [Open Fund project no. ZJUCEU2021008].

REFERENCES

(1) Zhao, S. L.; Pudasainee, D.; Duan, Y. F.; Gupta, R.; Liu, M.; Lu, J. H. A review on mercury in coal combustion process: Content and occurrence forms in coal, transformation, sampling methods, emission and control technologies. *Prog. Energy Combust.* **2019**, *73*, 26−64.

(2) Wu, Q. R.; Li, G. L.; Wang, S. X.; Liu, K. Y.; Hao, J. M. Mitigation options of atmospheric Hg emissions in China. *Environ. Sci. Technol.* **2018**, *52*, 12368−12375.

(3) Jia, T.; Ji, Z.; Wu, J.; Zhao, X. Y.; Wang, F. J.; Xiao, Y. X.; Qi, X. M.; He, P.; Li, F. T. Nanosized ZnIn2S4 supported on facet-engineered CeO2 nanorods for efficient gaseous elemental mercury immobilization. *J. Hazard. Mater.* **2021**, *419*, 126436.

(4) Cui, J.; Duan, L. B.; Jiang, Y.; Zhao, C. S.; Anthony, E. J. Migration and emission of mercury from circulating fluidized bed boilers co-firing petroleum coke and coal. *Fuel* **2018**, *215*, 638−646.

(5) Zhao, S. L.; Duan, Y. F.; Zhou, Q.; Zhu, C.; Liu, M.; Lu, J. H. Effects of NH4Br additive on mercury transformation and removal during CFB coal combustion. *J. Chem. Technol. Biotechnol.* **2017**, *92*, 391−398.

(6) Zhou, X.; Wu, J.; Li, Q. F.; Qi, Y. F.; Ji, Z.; He, P.; Qi, X. M.; Sheng, P. F.; Li, Q. W.; Ren, J. X. Improved electron-hole separation and migration in V2O5/rutile-anatase photocatalyst system with homo-hetero junctions and its enhanced photocatalytic performance. *Chem. Eng. J.* **2017**, *330*, 294−308.

(7) Zhao, S. L.; Duan, Y. F.; Lu, J. C.; Gupta, R.; Pudasainee, D.; Liu, S.; Liu, M.; Lu, J. H. Thermal stability, chemical speciation and leaching characteristics of hazardous trace elements in FGD gypsum from coal-fired power plants. *Fuel* **2018**, *231*, 94−100.

(8) Liu, D. J.; Li, C. E.; Wu, J.; Liu, Y. X. Novel carbon-based sorbents for elemental mercury removal from gas streams: A review. *Chem. Eng. J.* **2020**, *391*, 123514.

(9) Yang, Y. J.; Liu, J.; Zhang, B. K.; Liu, F. Mechanistic studies of mercury adsorption and oxidation by oxygen over spinel-type MnFe2O4. *J. Hazard. Mater.* **2017**, *321*, 154−161.

(10) Sun, P.; Zhang, B.; Zeng, X. B.; Luo, G. Q.; Li, X.; Yao, H.; Zheng, C. G. Deep study on effects of activated carbon's oxygen functional groups for elemental mercury adsorption using temperature programmed desorption method. *Fuel* **2017**, *200*, 100−106.

(11) Huang, T. F.; Duan, Y. F.; Luo, Z. K.; Zhao, S. L.; Geng, X. Z.; Xu, Y. F.; Huang, Y. J.; Wei, H. Q.; Ren, S. J.; Wang, H.; Gu, X. B. Influence of flue gas conditions on mercury removal by activated

carbon injection in a pilot-scale circulating fluidized bed combustion system. *Ind. Eng. Chem. Res.* **2019**, *58*, 15553−15561.
(12) Liu, H.; Chang, L.; Liu, W. J.; Xiong, Z.; Zhao, Y. C.; Zhang, J. Y. Advances in mercury removal from coal-fired flue gas by mineral adsorbents. *Chem. Eng. J.* **2020**, *379*, 122263.
(13) Liu, Y.; Bisson, T. M.; Yang, H. Q.; Xu, Z. H. Recent developments in novel sorbents for flue gas clean up. *Fuel Process. Technol.* **2010**, *91*, 1175−1197.
(14) Zamora, R. M. R.; Schouwenaars, R.; Moreno, A. D.; Buitron, G. Production of activated carbon from petroleum coke and its application in water treatment for the removal of metals and phenol. *Water Sci. Technol.* **2000**, *42*, 119−126.
(15) Xiao, Y.; Pudasainee, D.; Gupta, R.; Xu, Z. H.; Diao, Y. F. Elemental mercury reaction chemistry on brominated petroleum cokes. *Carbon* **2017**, *124*, 89−96.
(16) Xiao, Y.; Pudasainee, D.; Gupta, R.; Xu, Z. H.; Diao, Y. F. Bromination of petroleum coke for elemental mercury capture. *J. Hazard. Mater.* **2017**, *336*, 232−239.
(17) Chen, C.; Diao, Y. F.; Lu, Y.; Chen, S. S.; Tian, L. Complete reaction mechanisms of mercury binding on petroleum coke and brominated petroleum coke. *Energy Fuels* **2019**, *33*, 5488−5497.
(18) She, M.; Duan, Y. F.; Zhu, C.; Jia, C. Q. Impact of Nonoxidized Sulfur Species on Elemental Mercury Removal by SO2 Activated Petroleum Cokes. *Energy Fuels* **2020**, *34*, 14388−14399.
(19) Zhu, M. Q.; Yan, Q. T.; Duan, Y. F.; Li, J.; Zhang, X.; Han, Z. X.; Meng, J. L.; Wang, S. Y.; Chen, C.; Wei, H. Q. Study on preparation and mercury adsorption characteristics of columnar sulfur-impregnated activated petroleum coke. *Energy Fuels* **2020**, *34*, 10740−10751.
(20) Bisson, T. M.; Xu, Z. H. Potential hazards of brominated carbon sorbents for mercury emission control. *Environ. Sci. Technol.* **2015**, *49*, 2496−2502.
(21) Bisson, T. M.; Ong, Z. Q.; MacLennan, A.; Hu, Y. F.; Xu, Z. H. Impact of sulfur loading on brominated biomass ash on mercury capture. *Energy Fuels* **2015**, *29*, 8110−8117.
(22) Tzvetkov, G.; Mihaylova, S.; Stoitchkova, K.; Tzvetkov, P.; Spassov, T. Mechanochemical and chemical activation of lignocellulosic material to prepare powdered activated carbons for adsorption applications. *Powder Technol.* **2016**, *299*, 41−50.
(23) Do, J. L.; Friščić, T. Mechanochemistry: A force of synthesis. *ACS Cent. Sci.* **2017**, *3*, 13−19.
(24) Ma, A. J.; Zhao, S. L.; Luo, H.; Sun, Z. Q.; Sun, K.; Li, H. S. Mercury removal from coal-fired flue gas by the mechanochemical S/FeS modified high sulfur petroleum coke. *Fuel Process. Technol.* **2022**, *227*, 107105.
(25) Zhang, G. P.; Wang, Z. W.; Cui, L.; Zhang, X. Y.; Chen, S. Y.; Dong, Y. Efficient removal of elemental mercury from coal-fired flue gas over sulfur-containing sorbent at low temperatures. *ACS Omega* **2019**, *4*, 19399−19407.
(26) Ma, J. F.; Li, C. T.; Zhao, L. K.; Zhang, J.; Song, J. K.; Zeng, G. M.; Zhang, X. N.; Xie, Y. E. Study on removal of elemental mercury from simulated flue gas over activated coke treated by acid. *Appl. Surf. Sci.* **2015**, *329*, 292−300.
(27) Xu, Y.; Deng, F. F.; Pang, Q. C.; He, S. W.; Xu, Y. Q.; Luo, G. Q.; Yao, H. Development of waste-derived sorbents from biomass and brominated flame retarded plastic for elemental mercury removal from coal-fired flue gas. *Chem. Eng. J.* **2018**, *350*, 911−919.
(28) Li, H. L.; Zhu, W. B.; Yang, J. P.; Zhang, M. G.; Zhao, J. X.; Qu, W. Q. Sulfur abundant S/FeS2 for efficient removal of mercury from coal-fired power plants. *Fuel* **2018**, *232*, 476−484.
(29) Li, Y. N.; Duan, Y. F.; Wang, H.; Zhao, S. L.; Chen, M. M.; Liu, M.; Wei, H. Q. Effects of acidic gases on mercury adsorption by activated carbon in simulated oxy-fuel combustion flue gas. *Energy Fuels* **2017**, *31*, 9745−9751.
(30) Zhou, Q.; Duan, Y. F.; Chen, M. M.; Liu, M.; Lu, P.; Zhao, S. L. Effect of flue gas component and ash composition on elemental mercury oxidation/adsorption by NH4Br modified fly ash. *Chem. Eng. J.* **2018**, *345*, 578−585.
(31) Sun, Z.; Ma, A.; Zhao, S.; Luo, H.; Xie, X.; Liao, Y.; Liang, X. Research progress on petroleum coke for mercury removal from coal-fired flue gas. *Fuel* **2022**, *309*, 122084.
(32) Ma, Z. Z.; Deng, J. G.; Li, Z.; Li, Q.; Zhao, P.; Wang, L. G.; Sun, Y. Z.; Zheng, H. X.; Pan, L.; Zhao, S.; Jiang, J. K.; Wang, S. X.; Duan, L. Characteristics of NOx emission from Chinese coal-fired power plants equipped with new technologies. *Atmos. Environ.* **2016**, *131*, 164−170.
(33) Yang, Y. J.; Liu, J.; Wang, Z. Reaction mechanisms and chemical kinetics of mercury transformation during coal combustion. *Prog. Energy Combust.* **2020**, *79*, 100844.
(34) Shao, H. Z.; Liu, X. W.; Zhou, Z. J.; Zhao, B.; Chen, Z. G.; Xu, M. H. Elemental mercury removal using a novel KI modified bentonite supported by starch sorbent. *Chem. Eng. J.* **2016**, *291*, 306−316.
(35) Liu, Z. Y.; Yang, W.; Xu, W.; Liu, Y. X. Removal of elemental mercury by bio-chars derived from seaweed impregnated with potassium iodine. *Chem. Eng. J.* **2018**, *339*, 468−478.
(36) Wang, F. J.; Zhao, Y. F.; Zhang, M. L.; Wu, J.; Liu, G. L.; He, P.; Qi, Y. F.; Li, X. K.; Zhou, Y. Z.; Li, J. C. Bimetallic sulfides ZnIn2S4 modified g-C3N4 adsorbent with wide temperature range for rapid elemental mercury uptake from coal-fired flue gas. *Chem. Eng. J.* **2021**, *426*, 131343.
(37) Zhao, S. L.; Luo, H.; Ma, A. J.; Xie, W.; Sun, K.; Sun, Z. Q. Mercury removal by the S2Cl2 modified biomass coke with mechanochemical versus impregnation method. *Chem. Eng. J.* **2022**, *435*, 135073.
(38) Liu, H.; Yuan, B.; Zhang, B.; Hu, H. Y.; Li, A. J.; Luo, G. Q.; Yao, H. Removal of mercury from flue gas using sewage sludge-based adsorbents. *J. Mater. Cycles Waste Manage.* **2014**, *16*, 101−107.
(39) Geng, X. Z.; Hu, J. W.; Duan, Y. F.; Tang, H. J.; Huang, T. F.; Xu, Y. F.; Ren, S. J.; Liu, M. The effect of mechanical-chemical-brominated modification on physicochemical properties and mercury removal performance of coal-fired by-product. *Fuel* **2020**, *266*, 117041.
(40) Diamantopoulou, I.; Skodras, G.; Sakellaropoulos, G. P. Sorption of mercury by activated carbon in the presence of flue gas components. *Fuel Process. Technol.* **2010**, *91*, 158−163.
(41) Rumayor, M.; Diaz-Somoano, M.; Lopez-Anton, M. A.; Martinez-Tarazona, M. R. Mercury compounds characterization by thermal desorption. *Talanta* **2013**, *114*, 318−322.
(42) Rumayor, M.; Fernandez-Miranda, N.; Lopez-Anton, M. A.; Diaz-Somoano, M.; Martinez-Tarazona, M. R. Application of mercury temperature programmed desorption (HgTPD) to ascertain mercury/char interactions. *Fuel Process. Technol.* **2015**, *132*, 9−14.
(43) Zhao, S. L.; Duan, Y. F.; Lu, J. C.; Liu, S.; Pudasainee, D.; Gupta, R.; Liu, M.; Lu, J. H. Enrichment characteristics, thermal stability and volatility of hazardous trace elements in fly ash from a coal-fired power plant. *Fuel* **2018**, *225*, 490−498.
(44) Jia, L.; Yu, Y.; Li, Z. P.; Qin, S. N.; Guo, J. R.; Zhang, Y. Q.; Wang, J. C.; Zhang, J. C.; Fan, B. G.; Jin, Y. Study on the Hg0 removal characteristics and synergistic mechanism of iron-based modified biochar doped with multiple metals. *Bioresour. Technol.* **2021**, *332*, 125086.
(45) Lopez-Anton, M. A.; Rumayor, M.; Díaz-Somoano, M.; Martínez-Tarazona, M. R. Influence of a CO2-enriched flue gas on mercury capture by activated carbons. *Chem. Eng. J.* **2015**, *262*, 1237−1243.
(46) Yang, J. P.; Zhao, Y. C.; Chang, L.; Zhang, J. Y.; Zheng, C. G. Mercury adsorption and oxidation over cobalt oxide loaded magnetospheres catalyst from fly ash in oxyfuel combustion flue gas. *Environ. Sci. Technol.* **2015**, *49*, 8210−8218.
(47) Yang, J. P.; Zhao, Y. C.; Ma, S. M.; Zhu, B. B.; Zhang, J. Y.; Zheng, C. G. Mercury removal by magnetic biochar derived from simultaneous activation and magnetization of sawdust. *Environ. Sci. Technol.* **2016**, *50*, 12040−12047.
(48) Huo, Q. H.; Wang, Y. H.; Chen, H. J.; Han, L. N.; Wang, J. C.; Bao, W. R.; Chang, L. P.; Xie, K. C. ZnS/AC sorbent derived from the

https://doi.org/10.1021/acsomega.2c03449
ACS Omega 2022, 7, 31205−31217

high sulfur petroleum coke for mercury removal. *Fuel Process. Technol.* **2019**, *191*, 36−43.
(49) Zhao, S. L.; Duan, Y. F.; Yao, T.; Liu, M.; Lu, J. H.; Tan, H. Z.; Wang, X. B.; Wu, L. T. Study on the mercury emission and transformation in an ultra-low emission coal-fired power plant. *Fuel* **2017**, *199*, 653−661.
(50) Presto, A. A.; Granite, E. J.; Karash, A. Further investigation of the impact of sulfur oxides on mercury capture by activated carbon. *Ind. Eng. Chem. Res.* **2007**, *46*, 8273−8276.
(51) Duan, X. L.; Yuan, C. G.; Jing, T. T.; Yuan, X. D. Removal of elemental mercury using large surface area micro-porous corn cob activated carbon by zinc chloride activation. *Fuel* **2019**, *239*, 830−840.
(52) Tao, S. S.; Li, C. T.; Fan, X. P.; Zeng, G. M.; Lu, P.; Zhang, X.; Wen, Q. B.; Zhao, W. W.; Luo, D. Q.; Fan, C. Z. Activated coke impregnated with cerium chloride used for elemental mercury removal from simulated flue gas. *Chem. Eng. J.* **2012**, *210*, 547−556.

https://doi.org/10.1021/acsomega.2c03449
ACS Omega 2022, 7, 31205−31217